Current's Physical Components Theory and *p-q* Power Theory in the Control of the Three-phase Shunt Active Power Filter

Andrzej FIRLIT

AGH University of Science and Technology Cracow, POLAND

Summary: This paper presents the comparison among the control algorithms of a three phase, three wire shunt active power filter. The control algorithms are based on: 1) the current's physical components theory, 2) the *p-q* power theory. The active power filter operation under the distorted supply voltage at the point of common coupling condition is considered. The comparison concerns the aspects of: filtering current harmonics, reactive power compensation (defined in the fundamental harmonic domain), supply current balancing and dynamic performance. The results of the laboratory investigation, using the fast prototyping system dSPACE, are given in the paper. This paper confirms that the current's physical components theory allows developing the control algorithm of shunt active power filter and its practical implementation. The investigation allows the conclusion that this control algorithm enables achieving the supply system current shape close to the sinusoidal, despite shunt active power filter operation under the distorted supply voltage. A sinusoidal supply current cannot be attained by the control algorithm based on the *p-q* power theory without some additional control elements, such as: PLL, signal filters, etc. The experiment also has shown that the control algorithm based on the *p-q* power theory is easier to implement and less demanding in terms of hardware than the control algorithm based on the current's physical components theory.

1. INTRODUCTION

The active power filters (APFs) have been known as one of the best tools for harmonic mitigation as well as reactive power compensation, supply current balancing, voltage regulation and voltage flicker compensation etc. This wide range of objectives is achieved either individually or in combination, depending upon the requirements, a control algorithm (CA) and a configuration which have to be selected appropriately. One of the most popular APFs is shunt APF (SAPF), which is controlled to generate the required compensating currents. The control algorithm (CA) is one of the subsystems of the APF control system. The task of control algorithm is evaluation of reference signals on the grounds of information about voltages and currents at the point of common coupling (PCC). To obtain elimination of undesirable current components the applied control algorithm of SAPF has to evaluate properly the current components corresponding to higher harmonics, reactive power (defined in the fundamental harmonic domain) and the negative sequence components of the load current. The presence of distorted voltage at the PCC could affect evaluation of correct current components values. It depends on the chosen control algorithm. There are a number of methods that enable implementation of the control algorithm of SAPF, in a time or frequency domain. They are based on one of the power theories or the other approaches. This paper presents the comparison of the two control algorithms of SAPF under conditions of distorted voltage. They were designed on the basis of: the *p-q* power theory (PQT) and the current's physical components theory (CPCT). The first one was proposed by H. Akagi, A. Nabae and Y. Kanazawa [1–4], the second one was proposed by L.S. Czarnecki [9–12]. The PQT was developed in time domain, whereas the CPCT was developed in the frequency domain. The PQT is a well-known modern power theory and it is widely used in the field of active filtering, whereas the CPCT has been used in this area only once [9].

2. DESCRIPTION OF THE INVESTIGATED SYSTEM

The block diagram of the investigated three-phase three-wire SAPF system is shown in Figure 1. A thyristor rectifier, with *RL* load was used as a non-linear load. The resistor R_{uRS} was connected between the phases *R* and *S* in order to cause load currents asymmetry. SAPF configuration is based on a force-commutated pulse-width modulated voltage-source inverter (PWM-VSI) connected to a dc capacitor C_{APF}. The elimination of undesired load current components is achieved by injecting equal but of opposite sign compensating currents i_{APF}, which are generated by SAPF according to the chosen control algorithms. SAPF operation with the source non-zero internal impedance Z_S and for distorted voltage at the point of common coupling, resulting from the influence of other loads connected at the PCC, has been considered.

The current controller ensures constant switching frequency f_{sw}. It is essential considering the structure and effectiveness of the switching frequency filter, which eliminates the switching frequency component of SAPF current. A current controller, whose structure is presented in Figure 2, has been applied for this purpose [17, 18].
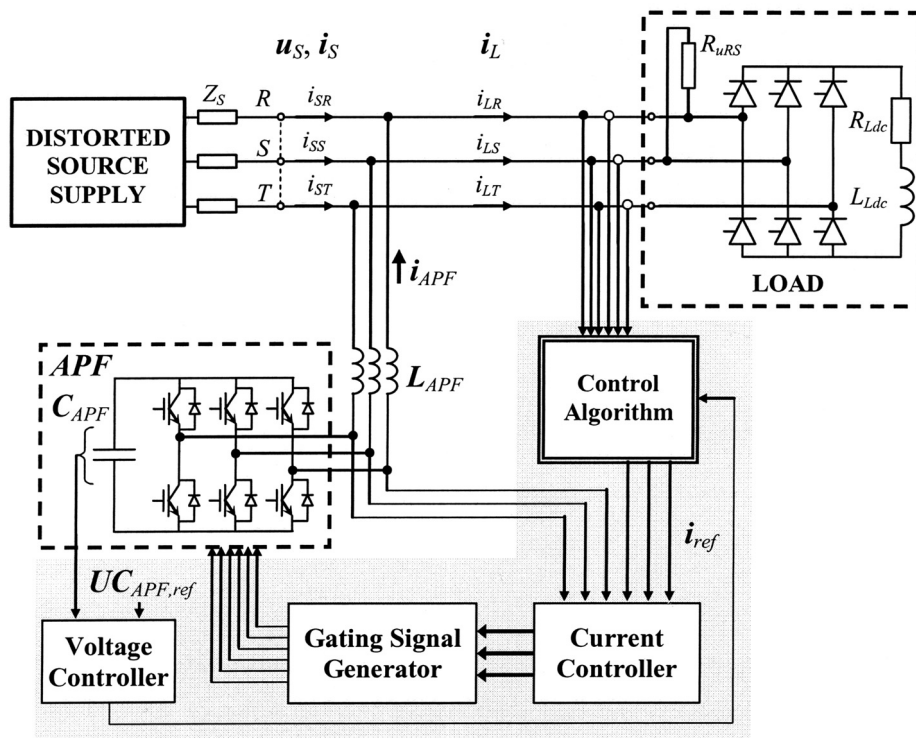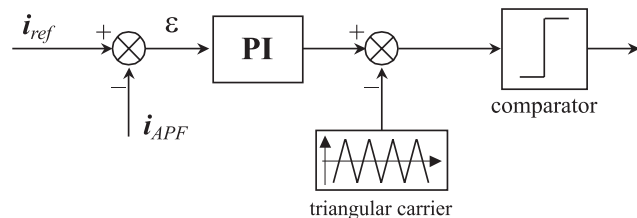
Fig. 1. The structure of the investigated SAPF

Fig. 2 The block diagram of the current controller

A constant switching frequency is achieved by comparing the current error signal ε with a triangular reference waveform. The purpose of introducing the triangular waveform is to stabilize the converter switching frequency by forcing it to be constant and equal to the frequency of the triangular reference signal. The error signal is processed through a PI controller before the comparison with the triangular carrier takes place. Switching of power SAPF produces the current ripples and also voltage ripples at the supply side because of non-zero internal source impedance Z_S. Voltage control of the dc bus is performed by adjusting the small amount of current flowing into the dc capacitor C_{APF}, thus compensating for both the converter and system losses [18].

3. CONTROL ALGORITHMS

According to the PQT, the current of the three-phase, unbalanced, non-linear load has been expressed into four components (Phase currents and voltages are expressed in the form of column vectors $i = i(t)$ and $u = u(t)$, where $\mathbf{i} = \left[i_R, i_S, i_T \right]^T$, $\mathbf{u} = \left[u_R, u_S, u_T \right]^T$):

$$i = i_{\bar{p}} + i_{\bar{q}} + i_h + i_{2f_{(1)}} \qquad (1)$$

where:

$p = \bar{p} + \tilde{p}_h + \tilde{p}_{2f_{(1)}}$ — instantaneous real power,

$q = \bar{q} + \tilde{q}_h + \tilde{q}_{2f_{(1)}}$ — instantaneous imaginary power ($\bar{p}, \bar{q}$ – average components, $\tilde{p}_h, \tilde{q}_h$ – oscillating components (h – "harmonic") and $\tilde{p}_{2f_{(1)}}, \tilde{q}_{2f_{(1)}}$ – oscillating components ($2f_{(1)}$ – with double frequency of the fundamental component frequency))

$i_{\bar{p}}$ — is associated with $\bar{p}$, i.e. with the active power P defined in the traditional way;

$i_{\bar{q}}$ — is associated with $\bar{q}$, i.e. with the reactive power Q (In the case of a symmetrical sinusoidal supply voltage and balanced load with or without harmonics, $\bar{q}$ is equal to the reactive power Q defined in the traditional way in the fundamental harmonic domain.);

i_h — is associated with $\tilde{p}_h$ and $\tilde{q}_h$, i.e. with the presence of harmonics in voltage and current waveforms;

$i_{2f_{(1)}}$ — is associated with $\tilde{p}_{2f_{(1)}}$ and $\tilde{q}_{2f_{(1)}}$, i.e. the unbalance load currents. The block diagram of the tested CA-PQT is shown in Figure 3a.

According to the CPCT, the current of the three-phase, unbalanced, non-linear load has been decomposed into five components:

$$i = i_a + i_s + i_r + i_u + i_B \qquad (2)$$

where:

i_a — active current,

i_s — scattered current,
i_r — reactive current,
i_u — unbalanced current
i_B — load generated current.

Each component is associated with a different power phenomenon and is orthogonal with respect to the others. Thus the current decomposition (2) reveals five different physical phenomena, which determine the load current value, namely: active energy transmission to the load – i_a; change of the load conductance $G_{e(n)}$ with frequency – i_s; reciprocating flow of energy – i_r; load currents unbalance – i_u; active energy transmission back to the source – i_B. If harmonic currents are generated by the supply source, due to the distorted voltage, then the current components i_a, i_s, i_r, i_u may contain, besides the fundamental, also high-order harmonics of the orders already present in the voltage (This is decided by the sign of the active power calculated for the given harmonic [11, 12]). Thus, each of the components i_a, i_s, i_r, i_u can be additionally decomposed into the fundamental and high-order harmonics, e.g.:

$$i_a = i_{a(1)} + i_{a(h)} \qquad (3)$$

where: the subscript (h) means the harmonics without the first harmonic. The subscript (1) means the first harmonic. The block diagram of the tested CA-CPCT is shown in Figure 3b.

The aim of SAPF is the elimination of all unwanted components of the load current from the point of view of the presented above current decompositions (1),(2). To achieve SAPF control objectives, the CAs have to generate the following reference current signals:
— according to the PQT (the control algorithm PQT – CA-PQT):

$$i_{refPQ} = i_{\bar{q}} + i_h + i_{2f_{(1)}} \qquad (4)$$

— according to the CPCT (the control algorithm CPCT – CA-CPCT):

$$i_{refCPC} = i_{a(h)} + i_s + (i_{r(1)} + i_{r(h)}) + (i_{u(1)} + i_{u(h)}) + i_B \quad (5)$$

4. EXPERIMENTAL RESULTS

The complete control system of SAPF consists of: a control algorithm unit, a current controller, a dc voltage controller, a gating signals generator, basic automation functions, etc. has been designed using the rapid prototyping system dSPACE and Matlab/Simulink environment. The developed SAPF control algorithms (CA-PQT, CA-CPCT) have been implemented and tested in the laboratory setup. The topology of the source–load path and SAPF is shown in Figure 1. The control systems of SAPF have been developed using dSPACE rapid prototyping system, consisting of:
— DS1005 processor board, with signal processor Motorola PowerPC 750, 480MHz,
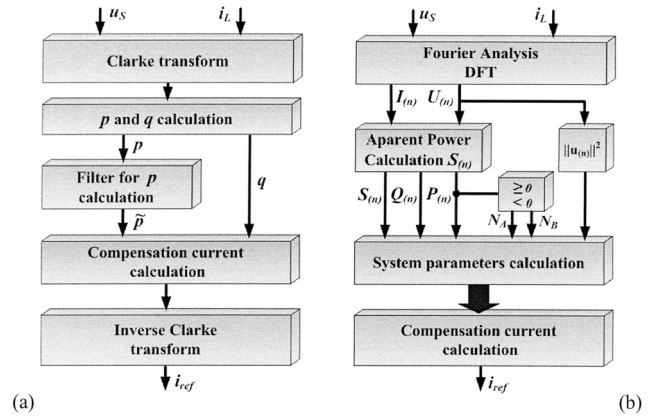— DS2002 Multi-Channel A/D board, 32 x 16-bit MUX, 2 ADCs, sim. S&H,

Fig. 3. The block diagrams of the control algorithms: (a) CA-PQT and (b) CA-CPCT

— Digital-I/O Board DS4003, 96 x dig. I/O,
— software: Matlab 5.3, Simulink 3.0, DSP Blockset 3.0 and Control DevelopmentPackage containing Real-Time Interface 3.5.1, ControlDesk 1.2.1, MTRACE/MLIB 4.1.

The main system parameters are:
— supply source:
  $U_S = 104/60$ V, $f_S = 50$ Hz
— internal impedance of supply source:
  $L_S \approx 0.25$ mH, $X_S \approx 79$ mΩ, $R_S \approx 7.9$ mΩ
— 6-pulse thyristor converter:
  $R_{Ldc} = 8.82\,\Omega$, $L_{Ldc} = 18.6$ mH,
  dc side and control angle: $\alpha_1 = 50°$, $\alpha_2 = 0°$
— resistive two-terminal network connected between the phases R and S:
  $R_{uRS} = 33.5\,\Omega$
— shunt active power filter:
  $L_{APF} = 1.9$ mH, $C_{APF} = 5$ mF, $UC_{APF,ref} = 320$ V
— switching frequency:
  $f_{sw} = 6.4$ kHz
— current PI controller:
  $K_p = 0.12$, $K_i = 153.0$
— UC_{APF} voltage PI controller:
  $K_{Cp} = 30.0$, $K_{Ci} = 53.2$

In the instantaneous real power p branch (PQT) was applied low-pass (LPF) Butterworth filter 2nd order with cut-off frequency $f_c = 25$Hz. The selected values result from a compromise between the accuracy of the load current unwanted components elimination and SAPF dynamic behavior. Application of relations formulated in CPCT requires that the complex values of amplitudes of $\underline{U}_{(n)}$ and $\underline{I}_{(n)}$ harmonics ($\underline{U}_{(n)} = [\underline{U}_{R(n)}, \underline{U}_{S(n)}, \underline{U}_{T(n)},]^T$, $\underline{I}_{(n)} = [\underline{I}_{R(n)}, \underline{I}_{S(n)}, \underline{I}_{T(n)},]^T$ being present in the measured voltage and current signals, shall be known. Therefore, in the first place the CPCT based control algorithm performs harmonic analysis of the supply voltage u_S and the load current i_L. In order to compute the current components and determine the reference current i_{refCPC}, a number of operations are performed on the set of the complex values of harmonics amplitudes, determined this way. In the investigation the complex amplitudes of harmonics $\underline{U}_{(n)}$ and $\underline{I}_{(n)}$ were determined using discrete Fourier transform DFT.

The DS2002 board limits the constant switching frequency to 6.4 kHz. This is due to a considerable A/D conversion time of the DS2002 board. With the applied 12-bit resolution, the
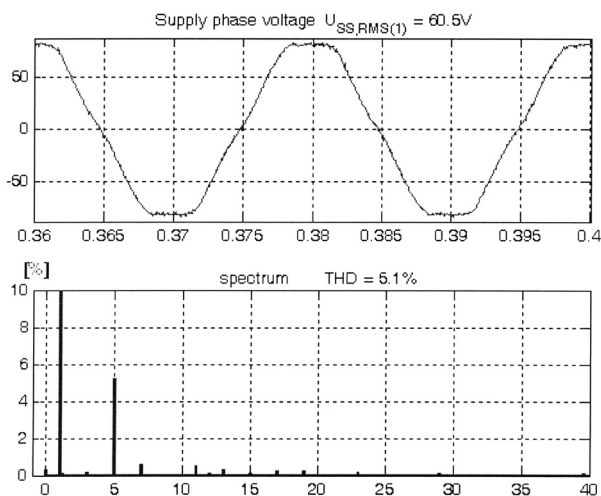
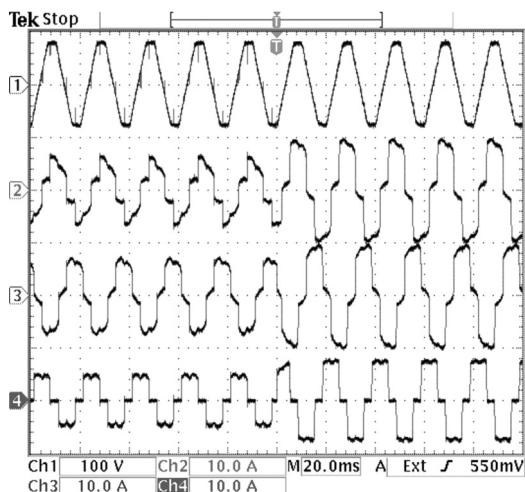Fig. 4. The waveform of supply voltage u_{SR} and its spectrum for phase R – unloaded source supply

Fig. 5. The waveforms of the supply voltage u_{SR} and the load phase currents i_{LR}, i_{LS}, i_{LT}

conversion time for a single channel is minimum $3.8\,\mu s$, and for 4 channels supported it gives $15.2\,\mu s$ (in the experiment 8 channel have been used, 4 per one converter). Also the time required for all computations associated with the control algorithm, as well as with the other elements of the control system, such as: current controller, dc voltage controller, basic

automation functions, etc. should be accounted for. The resulting sampling frequency was $f_s = 25.6$ kHz. For the obtained sampling frequency, a four times lower switching frequency has been defined f_{sw}, $(f_s/f_{sw} = 4)$. The control system CS-PQT has been developed using the Simulink standard blocks. The CS-CPCT has been developed using, apart of the Simulink blocks, also the DSP Blockset blocks. The time required to perform all computations for CS-PQT is successively ca. $26\,\mu s$, whereas for CS-CPCT this time is ca. $25.4\,\mu s$, depending on the 'quality' of the compilation carried out by dSPACE software. The computations for CS-PQT was performed in one time-loop, but for CS-CPCT in two time-loops: a master loop (T_{tt1}), identical for both control systems, restricted by the sampling time $T_s = 39.0625\,\mu s$, and the slave loop (T_{tt2}), which performs computations related solely to the CA-CPCT. Because of time restrictions, the number k of points DFT has been limited to $k = 32$. Thus, in the slave loop, for CA-CPCT, the value of reference current is updated every $625\,\mu s$ (20 ms/32) – during this time it is held at the constant value (Zero-Order-Hold block). The real time needed for all computations to be carried out in the slave loop is $325\,\mu s$, $300\,\mu s$ still remaining. However, the DSP Blockset toolbox DFT algorithm requires 2^k points. Increasing the number of points to $k = 64$, increases the duration of calculations and at the same time reduces the duration of calculations in the slave time-loop to $312.5\,\mu s$ (20 ms/64). This was beyond the capacity of the available dSPACE set.

The analysis of APF operation was carried out under conditions of a 'weak' supply system. Figure 4 shows the waveform and spectrum of the voltage $\boldsymbol{u}_S$, phase R, as observed at the terminals of unloaded supply source. The voltage $\boldsymbol{u}_S$ is distorted due to the adverse impact of other non-linear loads connected to the supply system. At the considered PCC this distortion varies within 4–6% $THD\boldsymbol{u}_S$.

Figure 5 shows in succession the waveform of the supply voltage u_{SR} and the waveforms of the load current $\boldsymbol{i}_L$ in steady state and dynamic state (step increase, $\alpha_1 = 50° \Rightarrow \alpha_2 = 0°$). The load current is asymmetrical, distorted and shifted in phase with respect to the voltage $\boldsymbol{u}_S$. The unbalance factor $UF\boldsymbol{i}_L$ is at the level 20.4% for $\alpha_1 = 50°$ and 12.0% for $\alpha_2 = 0°$.

The structure and parameters of the current controllers and the UC_{APF} voltage controllers were identical for both control algorithms. The values of the basic parameters of the investigated source-load path are given in Table 1.

The effects of SAPF operation in both the steady and dynamic states, for the developed SAPF control algorithms

Table 1. The values of the parameters before application of SAPF ($UF\boldsymbol{i}$ – unbalance factor).

phase		$\alpha_1 = 50°$			$\alpha_2 = 0°$		
		R	S	T	R	S	T
$THD\boldsymbol{i}_L$	%	24,84	22,03	30,00	23,74	23,26	28,28
I_L	A	8,50	10,28	7,52	14,18	14,34	11,77
DPF	–	0,887	0,734	0,661	-0,995	0,994	1,000
PF	–	0,856	0,713	0,627	-0,969	0,970	0,963
$UF\boldsymbol{i}_L$	%	20,40			12,00		

CA-PQT and CA-CPCT, are shown in Figure 6. Oscilloscope screen images show, consecutively, the waveforms of phase supply currents: i_{SR}, i_{SS}, i_{ST}.

Enlarged fragments of steady-state waveforms of the current i_{ST} (phase T, $\alpha_2 = 0°$), with its spectrum, are presented in Fig. 7 (left column). Subtracting the reference current i_{ref}, computed by the given CA, from the load current i_L we obtain the reference signal i_{Sref} for the current at the supply system side. The appropriate waveforms of the current i_{SrefT}, with its spectrum, are presented in Figure 7 (right column).

$$i_{Sref} = i_L - i_{ref} \qquad (6)$$

The values of basic parameters of the investigated SAPF system at the supply source side are given in Table 2.

From comparing the obtained waveforms of i_S current and the values presented in Table 2 it can be concluded that:
— the wave shapes of: i_{SPQ} and i_{SCPC} are close to each other and $THDi_S$ values are also close to each other.
— both CAs give the similar results in the supply current balancing.
— SAPF dynamic performance is closely comparable for both CAs. The obtained settling time in response to a step increase of the load current i_L is to 40 ms for both CAs.
— a difference occurs in the results of reactive power compensation. In the event of CA-CPCT, a phase shift occurs between the voltage u_S and current i_S due to the delay caused by the time needed for computing (slave time-loop – 625 μs $\Rightarrow$ 11,25° $\Rightarrow$ DPF = 0.981). Enlarged fragments of steady-state waveforms of: the supply voltage u_{SR}, the supply current i_{ST} and the reference current i_{SrefT} for CA-PQT and CA-CPCT are presented in Figure 8.
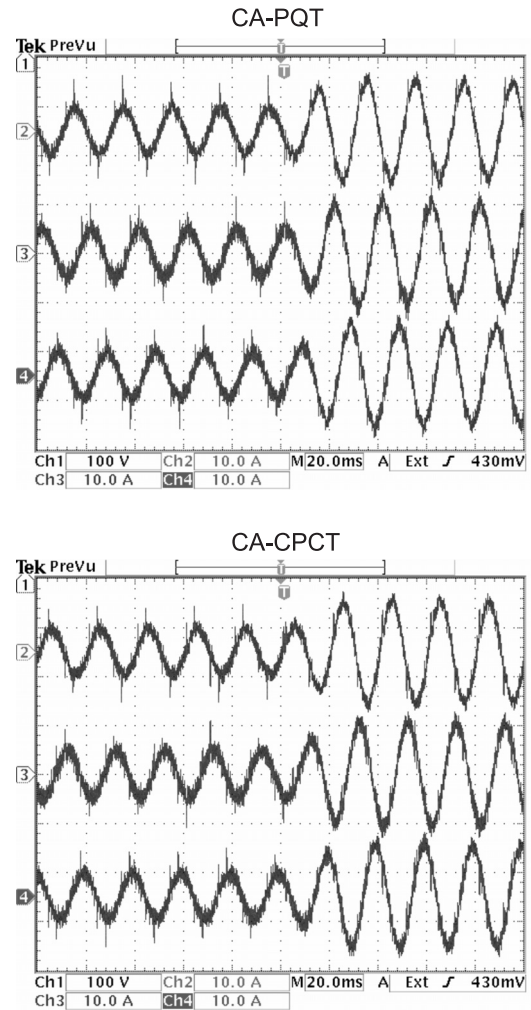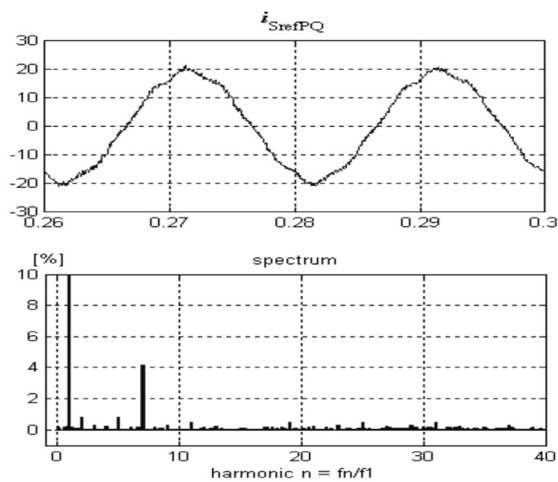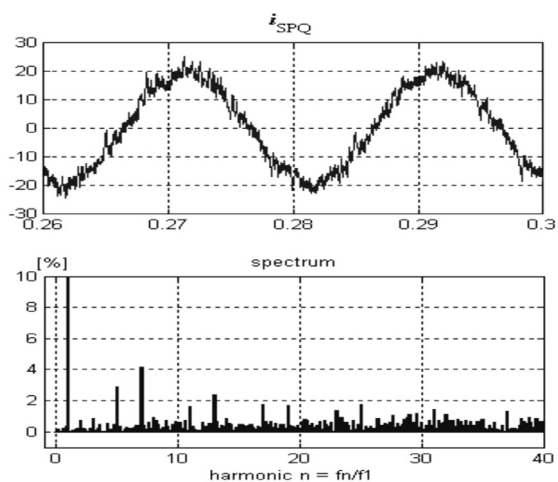

Fig. 6. The waveforms of current i_S for CA-PQT and CA-CPCT – experimental results (current scale × 2)

Table 2. The values of the parameters after application of SAPF (*UFi* – unbalance factor)

| phase		$\alpha_1 = 50°$			$\alpha_2 = 0°$		
		R	S	T	R	S	T
CS-PQT – turnaround time: $T_{tt1} = 26\mu$s							
$THDi_S$	%	18,15	16,52	15,65	10,62	9,15	9,33
I_S	A	7,27	7,30	7,26	13,60	13,74	13,61
DPF	–	-0,997	-0,998	-0,998	-0,999	-1,000	-1,000
PF	–	-0,966	-0,957	-0,965	-0,989	-0,988	-0,989
UFi_S	%	0,56			0,38		
CS-CPCT – turnaround times: $T_{tt1} = 25.4\mu$s, $T_{tt2} = 325\mu$s							
$THDi_S$	%	17,80	16,13	15,33	10,83	9,25	9,95
I_S	A	7,26	7,26	7,16	14,12	14,19	14,07
DPF	–	0,981	0,978	0,981	0,981	0,979	0,980
PF	–	0,950	0,938	0,948	0,970	0,966	0,969
UFi_S	%	0,65			0,48		

CA-PQT

CA-CPCT
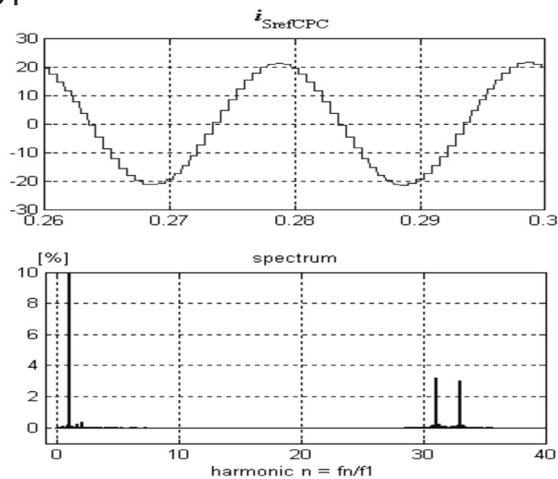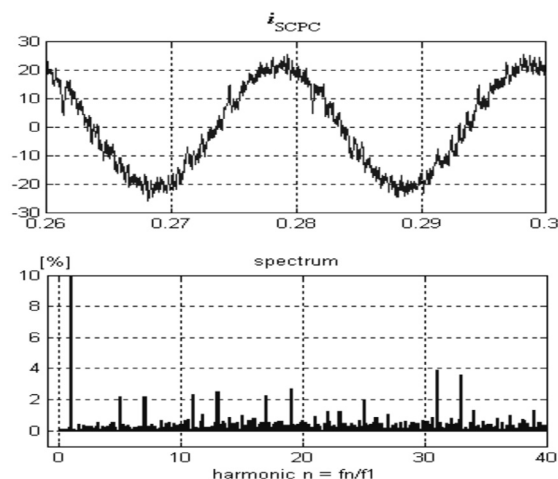
Fig. 7. Enlarged fragments of steady-state waveforms of current i_{ST} (left column) and i_{SrefT} (right column), with their spectra, for CA-PQT and CA-CPCT – experimental results
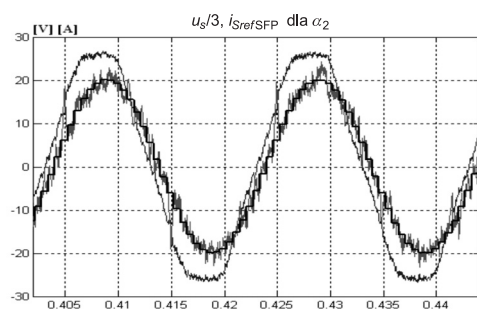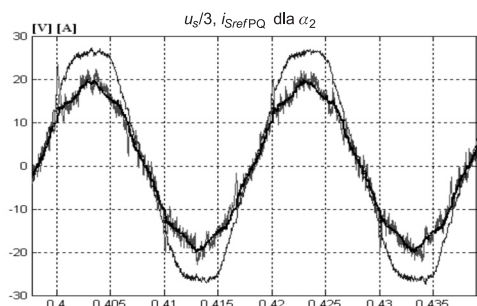

Fig. 8. Enlarged fragments of steady-state waveforms of: the supply voltage u_{ST}, the supply current i_{ST} and the reference current i_{SrefT} for: (a) CA-PQT, (b) CA-CPCT

The reference current signal i_{Sref} consists of the desired component of the load current i_L and the i_{APFdc} current, needed to replenish the C_{APF} capacitor energy, therefore:
— according to the CS-PQT:

$$i_{SrefPQ} = i_{\bar{p}} + i_{APFdcPQ} \qquad (7)$$

— according to the CS-CPCT:

$$i_{SrefCPC} = i_{a(1)} + i_{APFdcCPC} \qquad (8)$$

Figure 7 (right column) presents the example waveforms and spectra of currents i_{Sref} from relationships (7)–(8). Differences do occur between the currents i_S at the source side after applying SAPF and the currents i_{Sref} generated by the control systems for the given CA. This is a consequence of a relatively low switching frequency f_{sw} and the lack of passive filtering of the switching frequency component in SAPF current. The currents (7)–(8) differ between themselves, as well. The differences occur in both the wave shapes and in spectra. The current i_{SrefPQ} is distorted because of the voltage u_S distortion. In the current i_{SrefPQ} the 7th harmonic is dominant, though the 5th, 11th, 19th, etc. also occur. The

$i_{SrefCPC}$ current waveform approximates the sine-wave with the accuracy determined by the hardware capability. This is related to the above described method of CA-CPCT, where each subsequent value, computed by dSPACE, is updated every 625 μs. Hence, in the $i_{SrefCPC}$ spectrum, beside the first harmonic, also the 31st and 33rd harmonics occur. This is the cause of the $i_{SrefCPC}$ current distortion. Therefore the main cause of the $i_{SrefCPC}$ current distortion is not the supply voltage u_S distortion, but the hardware limitations. It ought to be emphasized that the CA-CPCT worked out the correct reference current i_{refCPC} in spite of the distorted supply voltage at the PCC. It was achieved without using the additional components of CA, such as PLL circuit, signal filter or others. The CA-CPCT was elaborated only on the grounds of the proposed physical interpretation of the phenomena occurring in electrical circuits and the mathematical relationships formulated within CPCT by L.S. Czarnecki.

5. CONCLUSIONS

In this paper the comparison of two control algorithms (CAs) of SAPF was presented. The CAs were designed on the basis of: the p-q power theory (PQT, CA-PQT) and the power theory based on the current's physical components theory (CPCT, CA-CPCT). The power theory based on the current's physical components took its final form in 1994 [12]. Until now, only its Author has presented proposals for this theory's practical application [9, 10]. This paper confirms that the power theory based on the current's physical components theory allows developing the control algorithm (CA-CPCT) of SAPF and its practical implementation. The CAs were implemented and tested using the fast prototyping system dSPACE. This hardware and software platform turned out to be a very useful tool for building and developing the control algorithms of SAPF. The laboratory results, with regard to the filtering current harmonics and supply current balancing, are similar for both control algorithms at the given switching frequency of SAPF f_{sw} = 6.4 kHz. Likewise the dynamic performance is comparable in the case of both CAs. The difference occurs in the results of reactive power compensation. In the event of CA-CPCT, a phase shift occurs between the voltage u_S and current i_S due to the delay caused by the time needed for computing (slave time-loop – 625 μs). Significant differences occur between the reference current signals i_{Sref} generated by the CAs. The reasons for the differences between the real i_S and the reference i_{Sref} currents at the source side after applying SAPF are that the laboratory setup has not been equipped with a passive filter for switching frequency elimination and a relatively low switching frequency f_{sw}. The investigation allows the conclusion that the developed algorithm CA-CPCT enables achieving the supply system current shape close to the sinusoidal, despite SAPF operation under the distorted supply voltage. A sinusoidal supply current cannot be attained by the CA-PQT without some additional control elements, such as: PLL, signal filters, etc. The experiment has shown that testing the capability of SAPF controlled by the CA-CPCT algorithm to its full extent requires a controller of a larger computing power.

This concerns both the A/D conversion time and harmonic analysis. An alternative solution is the use of a method for harmonic analysis of current and voltage signals different from the discrete Fourier transform DFT. The control algorithm CA-PQT, is certainly easier to implement and less demanding in terms of hardware.

LIST OF ABBREVIATIONS AND MAIN SYMBOLS

APF	— active power filter
CA	— control algorithm of shunt APF
CA-CPCT	— control algorithm of shunt APF based on the current's physical components theory
CA-PQT	— control algorithm of shunt APF based on the p-q power theory
CPCT	— current's physical components theory
CS-PQT	— control system of shunt APF with CA-PQT
CS	— control system of shunt APF
CS-CPCT	— control system of shunt APF with CA-CPCT
PCC	— point of common coupling
PQT	— p-q power theory
SAPF	— shunt APF
CPC	— in subscript – designation of CPCT, for example i_{refCPC}
PQ	— in subscript – designation of PQT, for example i_{refPQ}
R, S, T	— in subscript – designation of phases, for example i_{LR}, i_{LS}, i_{LT} – phase load currents
DPF	— displacement power factor
i, u	— vector of phase currents and voltages $i = [i_R, i_S, i_T]^T$, $u = [u_R, u_S, u_T]^T$,
i_{APF}	— SAPF current (current generated by SAPF)
i_{APFdc}	— current needed to replenish the C_{APF} capacitor energy
i_L	— load current
i_{ref}	— reference current (current generated by CA)
i_S	— supply current (current at the supply source side)
i_{Sref}	— reference signal for the current at the supply system side $i_{Sref} = i_L - i_{ref}$
PF	— power factor
THD	— total harmonic distortion
UF	— unbalance factor
u_S	— supply voltage

REFERENCES

1. A k a g i H . , K a n a z a w a Y . , N a b a e A .: *Instantaneous reactive power compensators comprising switching devices without energy storage components*. IEEE Trans. on Industry Applications, Vol. IA-20, No. 3, May/June 1984.
2. A k a g i H . , N a b a e A . , A t o h S .: *Control strategy of active power filters using multiple voltage-source PWM converters*. IEEE Trans. on Industry Applications, Vol. IA-22, No. 3, May/June 1986.
3. A k a g i H . , N a b a e A .: *The p-q theory in three-phase circuits under non-sinusoidal conditions*. Europ. Trans. on Electric Power, ETEP, Vol. 3, No. 1, pp. 27–31, 1993.
4. A k a g i H . , W a t a n a b e E . H . , A r e d e s M .: *The p-q theory for active filter control: some problems and solutions*. Sba Controle & Automação, Vol.15, No.1, pp. 78-84, ISSN 0103-1759, Jan./Mar. 2004.

5. A r e d e s   M . ,   H a f n e r   J .   H e u m a n n   K . : *Three-phase four-wire shunt active filter control strategies*. IEEE Transactions on Power Electronics, Vol. 12, No. 2, pp. 311–318, 1997.
6. B h a t t a c h a r y a   S . ,   D i v a n   D .   M . ,   B a n e r j e e   B . : *Synchronous Frame Harmonic Isolator Using Active Series Filter*. EPE'91, pp 3-030-3-035, Oct. 1991.
7. B h a t t a c h a r y a   S . ,   F r a n k   T .   M . ,   D i v a n   D .   M . ,   B a n e r j e e   B .: *Active Filter System Implementation*. IEEE Industry Application Magazine, pp. 47-63, September/October 1998.
8. C h u n g   S e - K y o : *A Phase Tracking System for Three Phase Utility Interface Inverters*. IEEE Transactions on Power Electronics, Vol. 15, No. 3, May 2000.
9. C z a r n e c k i   L . S . ,   C h e n   G . ,   S t a r o s z c z y k   Z . : *Application of running quantities for control of adaptive hybrid compensator*. European Trans. on Electrical Power, ETEP, Vol. 6, No. 5, pp. 337–344, 1996.
10. C z a r n e c k i   L . S . ,   H s u   S . M . ,   C h e n   G . : *Adaptive balancing compensator*. IEEE Trans. on Power Delivery, Vol. 10 No. 3, pp. 1663–1669, 1995.
11. C z a r n e c k i   L . S . : *Current and power equations at bidirectional flow of harmonic active power in circuits with rotating machines*. Europ. Trans. Electr. Power, Vol. 3, No. 1, pp. 45–52, ETEP 1993.
12. C z a r n e c k i   L . S . : *Dynamic, power quality oriented approach to theory and compensation of asymmetrical systems under nonsinusoidal conditions*. Europ. Trans. Electr. Power, 5, pp. 347–358, ETEP 1994.
13. E m a d i   A . ,   N a s i r i   A . ,   B e k i a r o v   S . B . : *Uninterruptible Power Supplies and Active Filters.* CRC Press, Illinois Institute of Technology, Chicago, USA, Power Electronics and Applications Series, Series edited by Muhammad H. Rashid, 2005.
14. F i r l i t   A . ,   S k a w i ń s k i   G . : *Comparison of control algorithms for three-phase three-wire shunt active power filter under distorted supply voltage using dSPACE system*. 8th International Conference Electrical Power Quality and Utilisation, Poland, Kraków, EPQU2003, pp. 303–311, 21–23.09.2005.
15. F i r l i t   A . : *The active power filter operation under the distorted supply voltage*. 11th International Conference EPE2005, Drezno, CD-No. 0686, 02–04.09.2005.
16. M o n t e i r o   L . F . C . ,   A r e d e s   M . : *A Comparative Analysis among Different Control Strategies for Shunt Active Filters*. in Proc. (CDROM) of the V INDUSCON – Conferęncia de Aplicaçőes Industriais, Salvador BA, Brazil, pp. 345–350, 03–05 July 2002.
17. M o r a n   L . ,   D i x o n   J . ,   W a l l a c e   R .: *A three-phase active power filter operating with fixed switching frequency for reactive power and current harmonic compensation*. IEEE Tran. on Power Industrial Electronics, Vol. 42, No 4, August 1995.
18. R a s h i d   M .   D i x o n   J . ,   M o r a n   L .: *Power Electronics Handbook, Chapter 33 Active Filters.* Academic Press, August 2001.

Andrzej Firlit

was born in Tarnów, Poland, in 1971. He received M.Sc. and Ph.D. degrees in electrical engineering from the AGH University of Science and Technology in Cracow, Poland, in 1996 and 2006, respectively. At present he is researcher in this University, in the Institute of Electrical Drive and Industrial Equipment Control. His areas of interest include power quality, power theories, active power filtering and computer analysis of power electronics systems.

Address:

AGH University of Science and Technology

Institute of Electrical Drive and Industrial Equipment Control

Al. Mickiewicza 30, 30-059 Cracow, Poland

phone: (+48) (0-12) 617-35-93

fax: (+48) (0-12) 633-22-84

e-mail: firlit@kaniup.agh.edu.pl